

# New Class of Scorpionate: Tris(tetrazolyl)–Iron Complex and Its Different Coordination Modes for Alkali Metal Ions

Ka Hyun Park,<sup>†,‡</sup> Kang Mun Lee,<sup>§,‡</sup> Min Jeong Go,<sup>†,‡</sup> Sung Ho Choi,<sup>||</sup> Hyoung-Ryun Park,<sup>†</sup> Youngjo Kim,<sup>\*,||</sup> and Junseong Lee<sup>\*,†</sup>

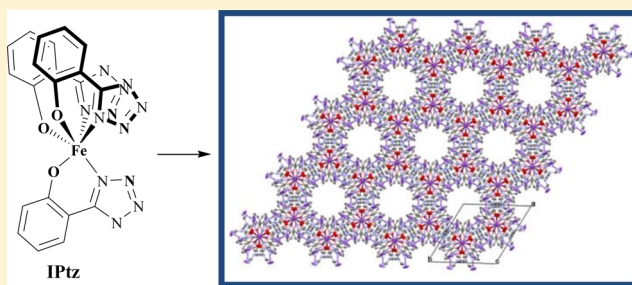
<sup>†</sup>Department of Chemistry, Chonnam National University, Gwangju 500-757, Korea

<sup>§</sup>Department of Chemistry, KAIST, Daejeon 361-763, Korea

<sup>||</sup>Department of Chemistry and BK21+ Program Research Team, Chungbuk National University, Cheongju, Chungbuk 361-763, Korea

## S Supporting Information

**ABSTRACT:** We report formation of a new metallascorpionate ligand,  $[\text{FeL}_3]^{3-}$  (IPTz), containing a Fe core and three 5-(2-hydroxyphenyl)-1H-tetrazole ( $\text{LH}_2$ ) ligands. It features two different binding sites, oxygen and nitrogen triangles, which consist of three oxygen or nitrogen donors from tetrazole. The binding affinities of the complex for three alkali metal ions were studied using UV spectrophotometry titrations. All three alkali metal ions show high affinities and binding constants ( $>3 \times 10^6 \text{ M}^{-1}$ ), based on the 1:1 binding isotherms to IPTz. The coordination modes of the alkali metals and IPTz in the solid were studied using X-ray crystallography; two different electron-donor sites show different coordination numbers for  $\text{Li}^+$ ,  $\text{Na}^+$ , and  $\text{K}^+$  ions. The oxygen triangles have the  $\kappa^2$  coordination mode with  $\text{Li}^+$  and  $\kappa^3$  coordination mode with  $\text{Na}^+$  and  $\text{K}^+$  ions, whereas the nitrogen triangles show  $\kappa^3$  coordination with  $\text{K}^+$  only. The different binding affinities of IPTz in the solid were manipulated using multiple metal precursors. A Fe–K–Zn trimetallic complex was constructed by assembly of an IPTz ligand, K, and Zn precursors and characterized using X-ray crystallography. Oxygen donors are coordinated with the K ion via the  $\kappa^3$  coordination mode, and nitrogen donors are coordinated with Zn metal by  $\kappa^3$  coordination. The solid-state structure was confirmed to be a honeycomb coordination polymer with a one-dimensional infinite metallic array, i.e.,  $-(\text{K}-\text{K}-\text{Fe}-\text{Zn}-\text{Fe}-\text{K})_n-$ .



## INTRODUCTION

Since the first introduction of tris(pyrazolyl)borates by Trofimenko in the 1960s, tridentate scorpionate ligands have received a great deal of attention, because of their structural diversity and wide range of applications in the field of supramolecular assembly, catalysis, and enzyme modeling.<sup>1</sup> Although many types of scorpionate ligand and their complexes have been reported in the literature, the search for new scorpionate systems is still of importance.<sup>2</sup> The reported strategies for synthesis of scorpionate ligands are as follows: (1) introduction of substituents at the 3 and/or 5 position(s) of the pyrazolyl rings, (2) production of neutral scorpionates by exchanging boron with carbon, (3) introduction of a fourth group bound to boron,<sup>3</sup> (4) exchange of pyrazolyl rings with five-membered triazolyl groups,<sup>4</sup> (5) exchange of pyrazolyl rings with six-membered pyridyl groups, (6) exchange of pyrazolyl rings with mercaptoimidazolyl<sup>5</sup> and thioxotriazolyl<sup>6</sup> moieties containing additional binding sites, and (7) exchange of pyrazolyl rings with mercaptothiadiazolyl, based on the geometric conformation that places all soft sulfur donors on one face of the ligand, directed toward the B–H moiety, and all

hard nitrogen donors on the opposite face, directed away from the hydride.<sup>7</sup>

Compared with the wide range of tris(pyrazolyl)borates and tris(triazolyl) borates available, examples of tris(tetrazolyl)borate systems are limited, although tetrazole and its derivatives have been widely used in the field of inorganic/coordination and materials chemistry, and a wide variety of new tetrazolyl–metal complexes based on Mn(II), Cu(II),<sup>8</sup> Co(II),<sup>9</sup> Fe(II),<sup>10</sup> Zn(II),<sup>11</sup> and Ti(IV)<sup>12</sup> have been reported in the literature. The first example of a tetrazolyl borate system, the bis(tetrazolyl)borate ligand, was reported by Janiak in the 1990s.<sup>13</sup> However, tris(tetrazolyl) borate systems, which are difficult to synthesize, were first reported by Winter and co-workers in 2013.<sup>14</sup> In this regard, a new synthetic approach for scorpionate ligands containing the tetrazole moiety is needed, and we paid attention to the fact that there is no example of a tris(tetrazolyl) metalloligand system reported. In addition, previously reported scorpionate systems have a boron center. We therefore focused on development of new metal-centered

Received: January 29, 2014

Published: July 30, 2014

scorpionate systems incorporating a Fe center; Fe is a versatile, cheap, and stable metal.

Very recently, we reported Ti complexes containing 5-(2-hydroxyphenyl)-1*H*-tetrazole (*LH*<sub>2</sub>), which is the sole example of a 5-substituted 1*H*-tetrazole containing a hydroxyl group,<sup>15</sup> in which *LH*<sub>2</sub> acted as a monoanionic bidentate ligand. Inspired by this, we envisioned that use of 5-(hydroxyphenyl)-1*H*-tetrazole (*LH*<sub>2</sub>) would lead to formation of metal complexes that possess a more complicated binding ability. In this article, we report a new class of alkali metal complexes, tris(tetrazolyl) metallascorpionates [*FeL*<sub>3</sub>]<sup>3-</sup> (IPTz), and its binding modes to Li<sup>+</sup>, Na<sup>+</sup>, and K<sup>+</sup>.

## RESULTS AND DISCUSSION

*LH*<sub>2</sub> was prepared using the known [2 + 3] azide cycloaddition.<sup>16</sup> The metallascorpionate complex **1** was prepared as an analytically pure solid by reaction of an H<sub>2</sub>O/DMF solution of Fe(ClO<sub>4</sub>)<sub>3</sub>·H<sub>2</sub>O with 3 equiv of *LH*<sub>2</sub> in the presence of NEt<sub>4</sub>OH. Because of the poor solubility of the tetrazole ligand, the reaction only proceeded under basic conditions. Compound **1** was characterized by mass spectroscopy data, IR, and elemental analysis that also suggested its formulation as [(NEt<sub>4</sub>)<sub>3</sub>FeL<sub>3</sub>]·3NEt<sub>4</sub>ClO<sub>4</sub> (**1**). Mass spectroscopy suggests that complex **1** possesses tris(tetrazolyl) metallascorpionate [*FeL*<sub>3</sub>]<sup>3-</sup> (IPTz) fragment in solution. Due to the paramagnetic nature of **1**, NMR spectroscopy was uninformative. We were unsuccessful at growing crystals suitable for X-ray diffraction studies.

**Binding Affinity Studies for Alkali Metal Ions.** To study the binding ability of IPTz for alkali metal ions, titration experiments using complex **1**, (NEt<sub>4</sub>)<sub>3</sub>FeL<sub>3</sub>, were performed. UV absorption spectra had absorption maxima at around 310 ( $\epsilon = 3 \times 10^4 \text{ M}^{-1} \text{ cm}^{-1}$ ) and 440 nm ( $\epsilon = 2 \times 10^3 \text{ M}^{-1} \text{ cm}^{-1}$ ), which were assigned as ligand-centered  $\pi-\pi^*$  transitions and ligand-to-metal charge transfer (LMCT) transitions of Fe, respectively.<sup>17</sup> On addition of complex **1** to an alkali metal perchlorate solution, an immediate color change from violet to reddish violet was observed.

To study the binding abilities of IPTz for alkali metal ions, the UV spectroscopic changes for the IPTz fragment on addition of an alkali metal perchlorate in MeCN were recorded (Figure 1). Spectra exhibited an absorption maximum shift (50 nm) on alkali metal ion addition, suggesting that the tetrazole ligands interact with the alkali metal ions. On addition of increasing amounts of alkali metal ion (0–1.5 equiv, Figure 1), the band at 440 nm was gradually quenched and a new absorption band at 480 nm ( $\epsilon = 2.8 \times 10^3 \text{ M}^{-1} \text{ cm}^{-1}$ , *M* = Li;  $1.6 \times 10^3 \text{ M}^{-1} \text{ cm}^{-1}$ , *M* = Na; and  $1.0 \times 10^3 \text{ M}^{-1} \text{ cm}^{-1}$ , *M* = K) was induced.

When LiClO<sub>4</sub> and NaClO<sub>4</sub> were added, the spectra did not change after the molar ratio of alkali metal ions to IPTz fragments reached 1:1 [bold red line in Figure 1A (LiClO<sub>4</sub>) and 1B (NaClO<sub>4</sub>)]. On the basis of the absorbance changes at 480 and 430 nm, the Li<sup>+</sup> and Na<sup>+</sup> ion binding constants (*K*) were estimated to be  $3 \times 10^6$  and  $1 \times 10^7 \text{ M}^{-1}$ , respectively, from the 1:1 binding isotherms. In contrast, in the case of KClO<sub>4</sub>, the absorption decreased even after the molar ratio of alkali metal ions to IPTz fragments reached 1:1 (bold red line in Figure 1C). Additional bindings between the nitrogen triangle and the K ions may be the main reason for the changes in the IPTz fragment spectrum. The K<sup>+</sup>-ion binding constants were estimated to be  $3 \times 10^7 \text{ M}^{-1}$ . The Job's plots suggest that complexes **1**–**3** formed 1:1 IPTz/alkali metal-ion complexes (Figures S12–S14, Supporting Information).

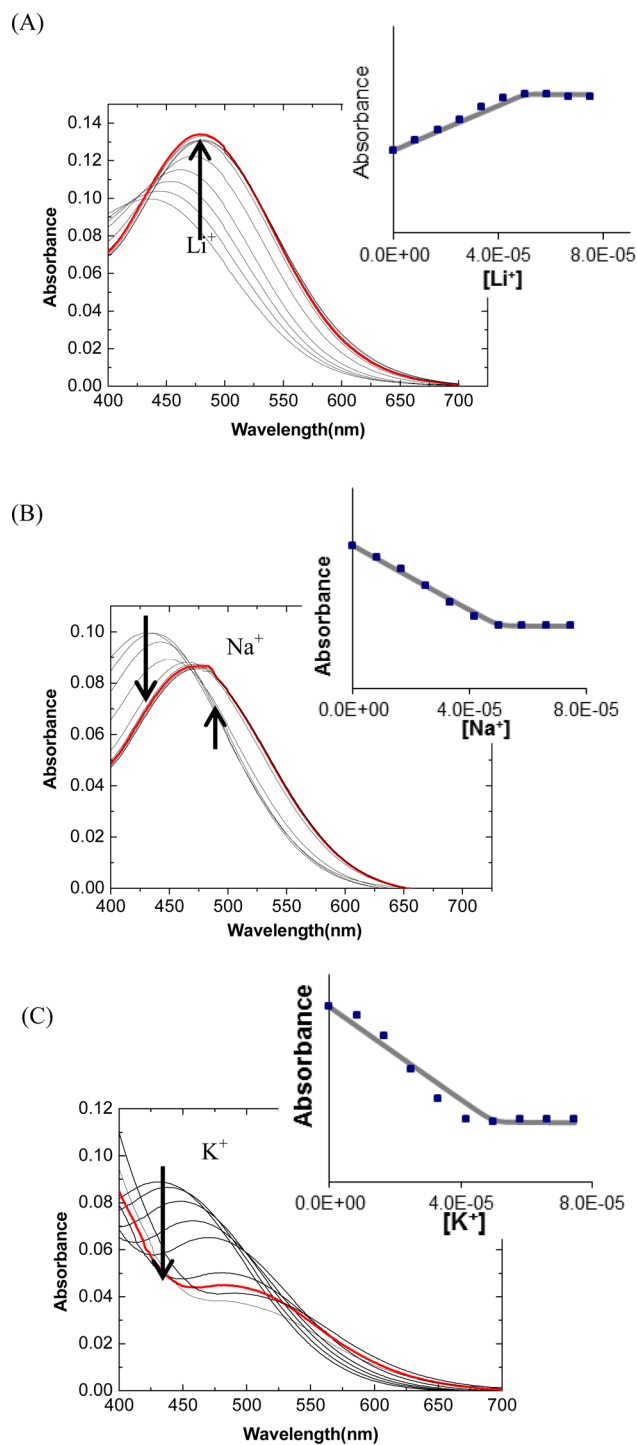


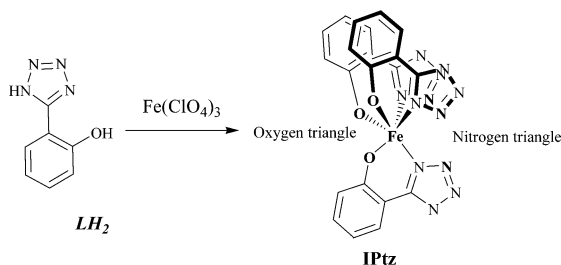
**Figure 1.** Changes in absorption spectra of complex **1** upon addition of alkali metal ions ( $1.67 \times 10^{-6} \text{ M}$ , 0–1.5 equiv): (A) Li<sup>+</sup>, (B) Na<sup>+</sup>, and (C) K<sup>+</sup> in MeCN at room temperature. The line corresponds to the binding isotherm calculated with  $3 \times 10^6 \text{ M}^{-1}$  for Li<sup>+</sup>,  $1.0 \times 10^7 \text{ M}^{-1}$  for Na<sup>+</sup>, and  $3.0 \times 10^7 \text{ M}^{-1}$  for K<sup>+</sup>.

**Solid-State Structures.** The bimetallic metallascorpionate complexes **2**–**4** were synthesized from H<sub>2</sub>O/DMF solutions of Fe(ClO<sub>4</sub>)<sub>3</sub>·H<sub>2</sub>O with 3 equiv of *LH*<sub>2</sub> in the presence of MOH (*M* = Li (**2**), Na (**3**), and K (**4**)). Fractional recrystallization from the mother liquor gave dark-violet crystals of **2**–**4** that were suitable for single-crystal X-ray diffraction. X-ray crystallography showed that their formulas in the solid state were [Li<sub>6</sub>Fe<sub>2</sub>L<sub>6</sub>(H<sub>2</sub>O)<sub>24.5</sub>]<sub>*n*</sub> (**2**), [Na<sub>3</sub>FeL<sub>3</sub>(H<sub>2</sub>O)<sub>9.5</sub>]<sub>*n*</sub> (**3**), and

$[K_3FeL_3(H_2O)_5]_n$  (**4**); these are consistent with the analytical data. Complexes **2–4** were soluble in  $H_2O$ , DMF, DMSO, MeOH, THF,  $CH_3CN$ , and acetone but were insoluble in  $Et_2O$ ,  $CH_2Cl_2$ , and hydrocarbons.

All three structures have the same metallascorpionate fragment, i.e., IPTz, which consists of three *L* ligands and one Fe atom (Scheme 1). The Fe center has  $C_3$ -symmetric

Scheme 1. Synthesis of IPTz



octahedral geometry, with three nitrogen atoms and three oxygen atoms of the *L* ligands. However, depending on the alkali metal used, the coordination modes between the Fe fragment and the alkali metal are totally different. IPTz has two different electron-donor sites,  $O_3$  and  $N_3$  triangles, defined by three oxygen and three nitrogen donors of IPTz (Scheme 1). It is worth noting that three oxygen atoms and tetrazole ligands are mutually disposed in facial positions, which may result from the thermodynamic trans effect in octahedral complexes.

X-ray photoelectron spectroscopy was used to investigate the oxidation states of the Fe ions in the complexes. The spectrum of complex **4** showed that it contained Fe(III) species (Figure S8, Supporting Information). The detailed spin state of the Fe ion was investigated using SQUID (superconducting quantum interference devices) magnetometry. The temperature dependences of  $\chi_M T$ , where  $\chi_M$  is the molar magnetic susceptibility and  $T$  is the temperature, are plotted in Figure S9, Supporting Information.  $\chi_M T$  values for **3** and **4** are around  $3.8$  and  $4.1$   $cm^3 mol^{-1} K$ , which are in the range for high-spin Fe(III) systems.<sup>17b,18</sup> In addition, the Fe–O and Fe–N bond distances are between  $1.9496(16)$  and  $1.9908(17)$  Å and  $2.0890(19)$  and  $2.1471(19)$  Å, respectively, also indicative of high-spin Fe(III) centers (Table 1).<sup>18,19</sup>

In the case of complex **2**, IPTz dimerizes in the solid state through two bridging Li ions between the two oxygens of the IPTz fragment and one nitrogen of the other IPTz fragment. The resulting  $C_i$ -symmetric dimer has four noncoordinating Li atoms, which are tetrahedrally surrounded by four  $H_2O$  molecules. Two types of Li-ion hydrates,  $Li(H_2O)_4$  and  $[Li_2(H_2O)_7]_{1/2}$ , were observed in the repeating unit. The structure formed a polymer of IPTz dimers via hydrogen bonds between  $Li(H_2O)_4$ ,  $Li_2(H_2O)_7$ ,  $H_2O$ , and IPTz.

One Li ion is coordinated with two oxygen atoms, and the Li–O distances are  $1.958$  and  $1.995$  Å. The distances between the oxygen atoms in the oxygen triangle defined by the oxygen donors of the tetrazole ligands are  $2.827(2)$ ,  $2.764(2)$ , and  $2.771(2)$  Å; it seems that this triangle is too large to bind the relatively small Li ion (ionic radius  $0.76$  Å)<sup>20</sup> by the  $\kappa^3$  coordination mode.

When NaOH was used as the alkali metal hydroxide, complex **3** was isolated. In compound **3**, the coordination modes of the Na ions and IPTz fragments are more complicated. The Na ion (radius  $1.02$  Å<sup>20</sup>) is able to bind to the oxygen

Table 1. Selected Bond Distances (Angstroms) for Complexes **2–5**

	2	3	4	5
Fe–O	1.9496(16)	1.9361(15)	1.935(6)	1.953(5)
	1.9563(16)	1.9529(15)	1.941(6)	
	1.9893(17)	1.9779(16)	1.979(7)	
	1.9460(16)			
	1.9660(16)			
	1.9908(17)			
	2.0939(19)	2.1038(18)	2.119(8)	2.134(6)
	2.0990(19)	2.1296(17)	2.119(8)	
	2.115(2)	2.1471(19)	2.140(8)	
	2.0890(19)			
2.124(2)				
Fe–M	2.883(4)	3.0764(3)	3.3310(15)	3.444(4)
	2.900(4)		4.489(2)	
M–O <sub>L</sub>	1.958(4)	2.4129(14)	2.697(6)	2.831(5)
	1.995(4)	2.3810(17)	2.704(7)	
	1.961(4)	2.7300(17)	2.843(6)	
	1.995(4)			
M–N <sub>L</sub>	1.997(4)	2.437(2)	2.825(9)	2.155(6)
	2.029(4)		2.952(8)	
			2.848(8)	
			2.958(9)	
			3.183(9)	
M–Ph			3.116(9)	
			3.054(9)	
			3.725(9)	

triangle by the  $\kappa^3$ - $O_3$  coordination mode. The Na–O bond lengths are  $2.4129(14)$ ,  $2.3810(17)$ , and  $2.7300(17)$  Å. As a result, the structure has a relatively short Fe–Na distance ( $3.0764$  Å). This central Na ion is involved in  $\kappa^6$ - $O_6$  coordination with two oxygen triangles defined by the oxygen donors of tetrazole ligands. This coordination results in formation of a Na sandwich complex with the sequence IPTz–( $\kappa^3$ - $O_3$ )–Na–( $\kappa^3$ - $O_3$ )–IPTz. The side lengths of the  $O_3$  triangle of the IPTz fragment are  $2.723(2)$ ,  $2.740(2)$ , and  $2.787(2)$  Å, and the  $N_3$  triangle of the IPTz fragment has side lengths of  $3.435(2)$ ,  $3.772(2)$ , and  $3.574(2)$  Å and is still too large to interact tightly with Na.

Complex **3** also formed a polymeric structure. Na<sub>2</sub>, Na<sub>3</sub>, and Na<sub>4</sub> form a triangle via O<sub>6</sub>, O<sub>7</sub>, O<sub>8</sub>, and O<sub>12</sub>  $H_2O$  molecules, and the triangles are connected by O<sub>4</sub> and O<sub>5</sub>  $H_2O$  molecules, forming a chain. This chain is linked by Na<sub>2</sub>–IPTz–Na<sub>1</sub>–IPTz–Na<sub>2</sub> coordination. Additional coordination among Na, tetrazole, and  $H_2O$  molecules results in formation of a three-dimensional structure.

Complex **4**, incorporating K ions, which have a bigger radius than Li and Na ions, was synthesized using KOH as a base. The structure of **4** is similar to that of **3**, but higher coordination numbers between the metal atom and the nitrogen side of IPTz were observed. As already observed for complex **3**, the K ion of the oxygen side is sandwiched by two  $\kappa^3$ - $O_3$  atoms of IPTz, giving octahedral geometry. K–O bond lengths are  $2.697(6)$ ,  $2.843(6)$ , and  $2.704(7)$  Å. This coordination results in formation of a K–Fe–K sequence. The  $N_3$  plane of the IPTz fragments is also connected to K ions by  $\eta^3$ - $N_3$  coordination. Moreover, tetrazole ligands have additional coordination with alkali metal ions, forming  $\kappa^5$  and  $\kappa^2$  coordination modes with K<sub>3</sub> and K<sub>4</sub>, respectively. The K–N bond lengths are between

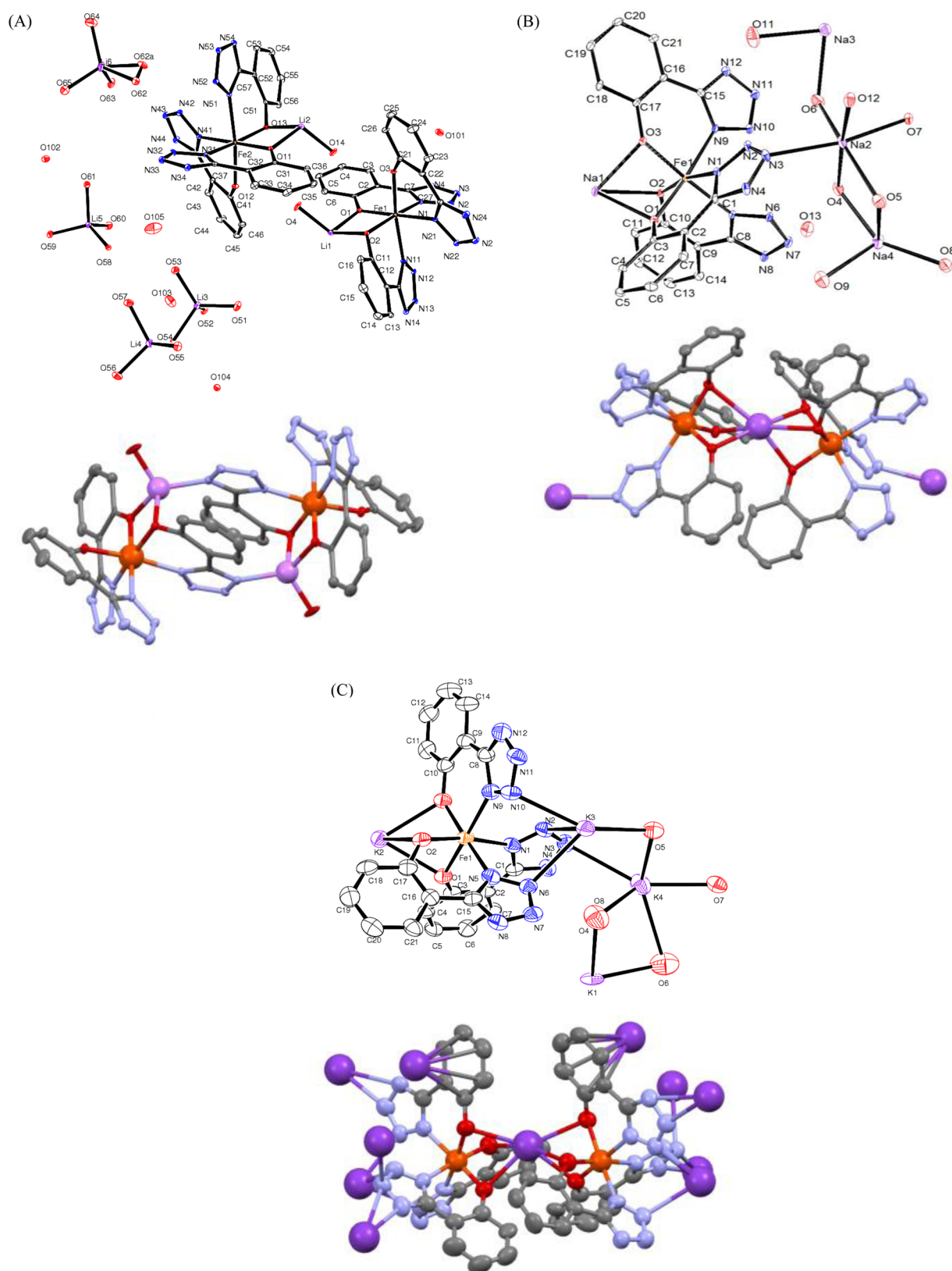


**Figure 2.** ORTEP diagrams and binding of metal ions (2, Li; 3, Na; 4, K) and IPTz in complexes (A) 2, (B) 3, and (C) 4. H atoms, H<sub>2</sub>O molecules, and free metal ions are omitted for clarity. Color code: orange = Fe; purple = alkali metal ion; red = O; and sky blue = N.

2.848(8) and 2.958(9) Å, which are longer than those of K–O. These coordination modes extend the coordination sequence of metals and IPTz to K–( $\kappa^3$ -N<sub>3</sub>)–FeL<sub>3</sub>–( $\kappa^3$ -O<sub>3</sub>)–K–( $\kappa^3$ -O<sub>3</sub>)–FeL<sub>3</sub>–( $\kappa^3$ -N<sub>3</sub>)–K (Figure 2).

Interestingly,  $\pi$  bonding between K and the phenyl group of tetrazole was observed. The distances between K and the phenyl ring were 3.054(9) and 3.725(9) Å. It is worth noting that there are only a few reported examples of mixed-metal



complexes containing ligands as both  $\sigma$  and  $\pi$  donors.<sup>21</sup> The IPTz fragment has quite short distances, 3.3309(15) and 4.489(2) Å, between Fe and K located on the nitrogen side and K located on the oxygen side, respectively (Figure 3).

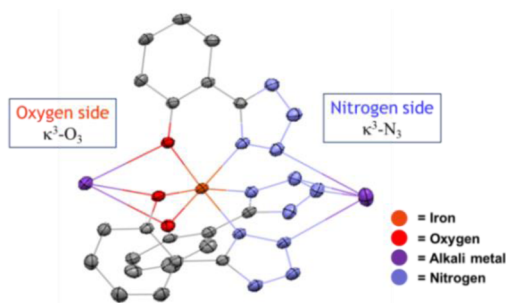


**Figure 3.** Binding of two K atoms and IPTz in complex 4. Color code: orange = Fe; purple = K; red = O; and sky blue = N.

Complex 4 also forms a polymeric structure. K1 and K4 form a  $[K_4O_4]$ -type dimer along the (110) plane via O5 and O6  $H_2O$  molecules. K3 and N6 and N7 of the tetrazole form a square along the (110) plane. The K3 and K4 atoms of two squares are connected by an O5  $H_2O$  molecule and tetrazole, growing in the  $[110]$  direction. This chain is again linked by K3–IPTz–K2–IPTz–K3. By means of addition coordination among K, tetrazole, and  $H_2O$  molecules, it forms a three-dimensional structure.

Comparison of coordination modes of IPTz with alkali metals is listed in Table 2. This result indicates that the coordination

**Table 2.** Coordination Modes of Alkali Metal Ions with IPTz in the Crystal Structure

complex	alkali metal	oxygen site	nitrogen site
2	Li	$\kappa^2$	$\kappa^1$
3	Na	$\kappa^3$	$\kappa^1$
4	K	$\kappa^3$	$\kappa^3 + \kappa^2, \kappa^2$

modes of the oxygen triangle and nitrogen triangles of IPTz are totally different. The small oxygen triangle is coordinated with alkali metal ions with multiple coordination numbers, but K ions are only coordinated with multiple coordination numbers to the nitrogen triangle of IPTz. It seems that in complex 4 the K ions are sufficiently large to coordinate with three nitrogen and three oxygen atoms of IPTz. The K–O bond lengths are significantly larger than the Na–O bond lengths. This probably makes the tetrazole ligands more flexible and provides smaller nitrogen triangle sides. As a result, the  $N_3$  triangle has side lengths of 3.342(2), 3.391(2), and 3.742(2) Å and a high coordination number with K ions.

We performed ESI-mass spectrometry for the three newly synthesized complexes and confirmed the presence of bimetallic IPTz fragments in solution.

The electrochemical properties of IPTz were investigated using cyclic voltammetry (CV; Figures S10 and S11, Supporting Information). The results show that complexes 1–4 undergo one irreversible oxidation at 0.8–1.2 V (vs Ag/AgCl), which is in a similar range to that observed for Fe(III) complexes, confirming formation of Fe(III) complexes.<sup>22</sup>

**Formation of Trimetallic Three-Dimensional Coordination Polymer.** Finally, based on the successful preparation of bimetallic assemblies and the Janus-type nature of the

ligands, we further explored the possibility of making a trimetallic assembly in which a hard Lewis acid,  $K^+$ , would bind with hard phenolate oxygens and an intermediate Lewis acid,  $Zn^{2+}$ , would bind to the softer tetrazolyl groups. A heterometallic polymeric system using both ends of the metallascorpionate ligand was prepared using multiple metal precursors

A mixture of iron and zinc perchlorates in the presence of KOH,  $NH_4OH$ , and  $LH_2$  in DMF yielded the novel three-dimensional trimetallic coordination polymer complex  $[K_4Zn(FeL_3)_2(DMF)_6]_n$  (5; Figure 4). This complex also has an IPTz fragment in which the oxygen and nitrogen sides are connected to K and Zn ions via  $\eta^3-O_3$  and  $\eta^3-N_3$  coordination, respectively. K–O and Zn–N bond lengths are 2.831(5) and 2.155(6) Å, respectively. Metal ions are located on a 3-fold rotational axis, forming a one-dimensional infinite metallic array  $-(K-K-Fe-Zn-Fe-K)_n-$ .

Extension of the asymmetric unit of complex 5 resulted in a honeycomb structure and vacant holes (diameter = 10.2 Å); these would be useful for selective absorption of gases such as  $N_2$  and  $CO_2$  (Figure 5). A detailed study of the gas absorption properties of complex 5 is in progress.

## CONCLUSIONS

We prepared and characterized a new tris(tetrazolyl)–Fe metallascorpionate system, IPTz. Its binding modes to alkali metals in the solid state are highly dependent on the alkali metal used, as shown by solid-state structural analysis. By means of strong interactions between two K ions and three L ligands ( $\kappa^3-O$  and  $\kappa^3-N_3$ ) the complex forms a sandwich-like structure with the sequence K–FeL<sub>3</sub>–K with short Fe–K distances. The binding affinities of the IPTz fragments to alkali metal ions were very strong with high binding constants ( $>1 \times 10^6 M^{-1}$ ); these were investigated using titration experiments. A honeycomb-structured coordination polymer with a one-dimensional infinite metallic array, i.e.,  $-(K-K-Fe-Zn-Fe-K)_n-$ , was constructed by assembly of tetrazole and K, Fe, and Zn precursors.

## EXPERIMENTAL SECTION

**General Considerations.** Anhydrous-grade solvents (Aldrich) were dried by passing them through an activated alumina column; they were stored over activated molecular sieves (5 Å). All commercial chemicals were purchased from Aldrich and used without further purification.

**Measurements.** Elemental and mass analyses were performed using an EA 1110-FISONS (CE) at KAIST and a high-resolution ESI-MS instrument at the KBSI Ochang Center. IR spectra were obtained using KBr pellets with a Bruker EQUINOX-55 spectrophotometer. UV–vis absorption spectra were recorded using a Jasco V-530 instrument. Magnetic susceptibility measurements were carried out at the Korea Basic Science Institute in Seoul using a Quantum Design MPMS-7 SQUID magnetometer.

**[(NET<sub>4</sub>)<sub>3</sub>FeL<sub>3</sub>·3NET<sub>4</sub>ClO<sub>4</sub> (1).** A mixture of  $LH_2$  (0.9 mmol, 0.146 g) and iron(III) perchlorate hydrate (0.3 mmol, 0.106 g) was added to a mixture of  $NET_4OH$  solution (2.78 M, 0.648 mL) and  $H_2O$  (1 mL) in a 10 mL vial and stirred for 5 h. Slow evaporation of the solvents yielded a dark-purple solid within 2–3 weeks [88% yield, based on Fe(III)]. Anal. Calcd (Found) for  $C_{69}H_{132}N_{18}O_{15}FeCl_3$ : C, 51.28 (51.47); H, 8.23 (8.20); N, 15.60 (14.20). Selected IR data ( $cm^{-1}$ , KBr pellet): 3420 [s, br,  $\nu(O-H)$  of  $H_2O$ ], 2952 [m,  $\nu(L^{2-})$ ], 1627 (m), 1589 [m,  $\nu(L^{2-})$ ], 1555 [w,  $\nu(L^{2-})$ ], 1466 [s,  $\nu(L^{2-})$ ], 1441 (m,  $ClO_4^-$ ), 1312 [m,  $\nu(L^{2-})$ ], 1255 (m), 1098 (s,  $ClO_4^-$ ), 1005 (w), 855 [m,  $\nu(Fe-O)$ ], 829 (m), 765 (m), 671 (m), 624 [m,  $\nu(Fe-O)$ ], 562 [m,  $\nu(Fe-N)$ ], 478 (m).

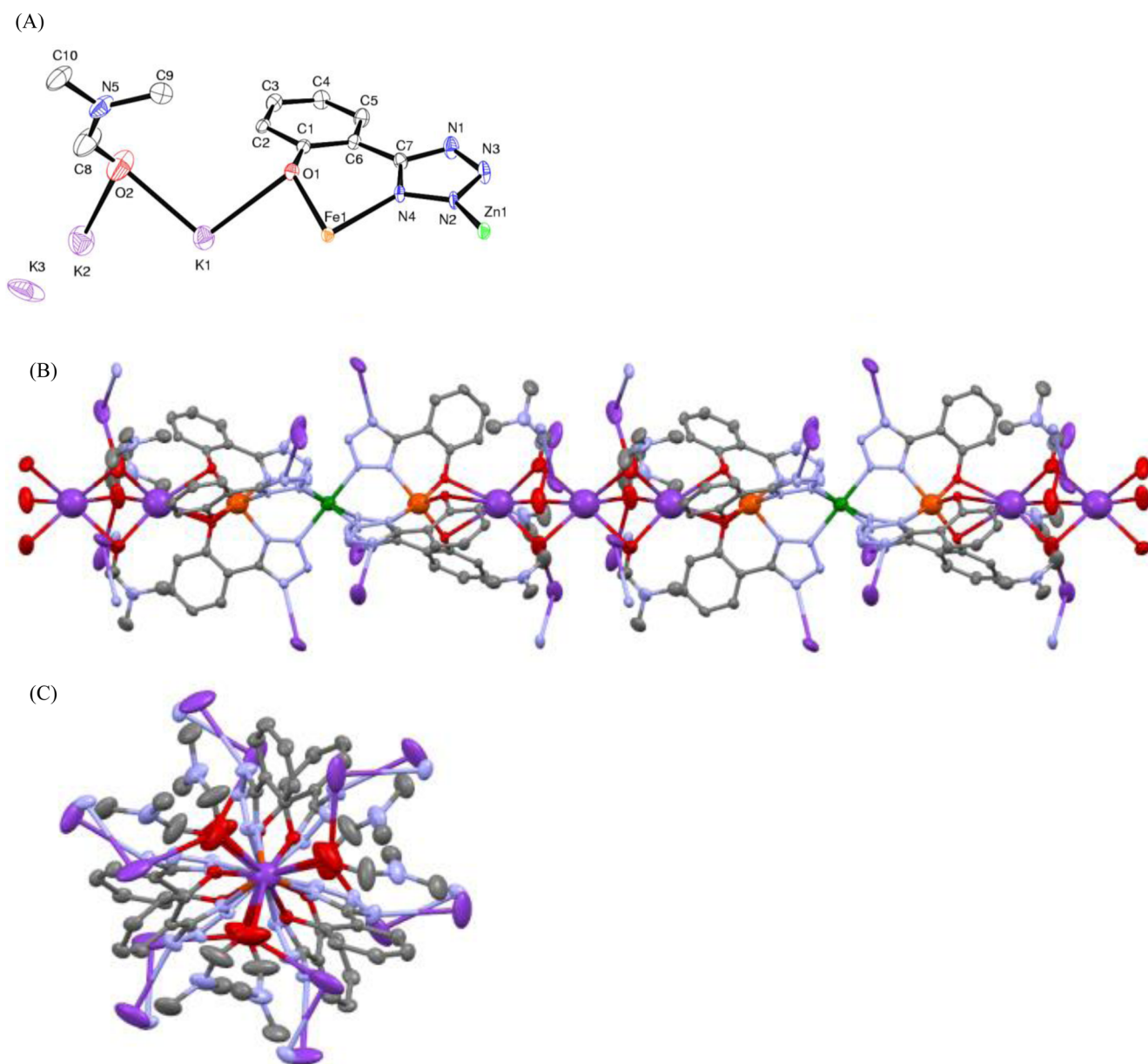


**Figure 4.** Asymmetric unit (A), and extended view along the *ac*-plane (B) and down the  $C_3$  axis (C) of the solid-state structure of **5**.

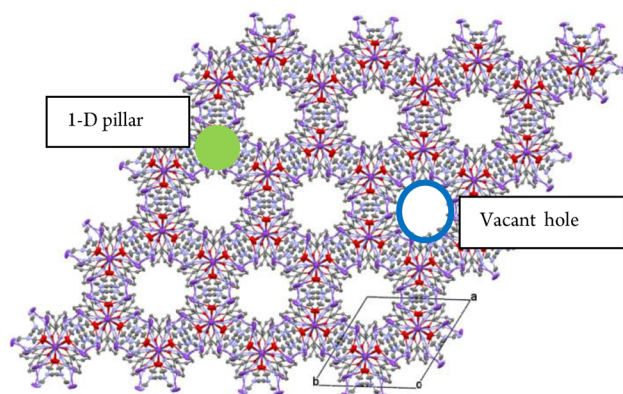


**Figure 5.** Extended structure of **5**, looking down the *c* axis.

**[Li<sub>6</sub>Fe<sub>2</sub>L<sub>6</sub>(H<sub>2</sub>O)<sub>24.5</sub>] (2).** A mixture of  $LH_2$  (0.3 mmol, 0.0486 g) and iron(III) perchlorate hydrate (0.3 mmol, 0.106 g) was added to a mixture of aqueous LiOH solution (0.500 M, 2 mL) and DMF (2 mL)

in a 10 mL vial. Slow evaporation of the solvents yielded dark-purple crystals [65% yield, based on Fe(III)]. Anal. Calcd (Found) for  $Li_6C_{42}H_{67}N_{24}O_{27.5}Fe_2$ : C, 33.60 (33.76); H, 4.50 (4.48); N, 22.39 (22.93). Selected IR data ( $cm^{-1}$ , KBr pellet): 3467 [s, br,  $\nu(O-H)$  of  $H_2O$ ], 2924 [m,  $\nu(L^{2-})$ ], 1647 (m), 1601 [m,  $\nu(L^{2-})$ ], 1565 [w,  $\nu(L^{2-})$ ], 1509 [w,  $\nu(L^{2-})$ ], 1468 [s,  $\nu(L^{2-})$ ], 1299 [m,  $\nu(L^{2-})$ ], 1269 [m,  $\nu(Li-O)$ , O of  $H_2O$ ], 1242 [m,  $\nu(Li-O)$ , O of  $H_2O$ ], 1145 (s), 1089 [s,  $\nu(L^{2-})$ ], 1018 (w), 941 [w,  $\nu(Fe-O)$ ], 853 [m,  $\nu(Fe-O)$  and  $(L^{2-})$ ], 755(m), 671 (m), 627 [s,  $\nu(Fe-O)$ ], 571 (m), 489 [m,  $\nu(Fe-N)$ ].

**[Na<sub>3</sub>FeL<sub>3</sub>(H<sub>2</sub>O)<sub>9.5</sub>] (3).** A mixture of  $LH_2$  (0.9 mmol, 0.146 g) and iron(III) perchlorate hydrate (0.3 mmol, 0.106 g) was added to a mixture of aqueous NaOH solution (0.500 M, 2 mL) and DMF (2 mL) in a 10 mL vial and stirred for 5 h. Slow evaporation of the solvents yielded a dark-purple solid within 2–3 weeks [51% yield, based on Fe(III)]. Anal. Calcd (Found) for  $Na_3C_{21}H_{18}N_{12}O_6Fe$ : C, 38.26 (38.62); H, 2.75 (2.74); N, 25.50 (25.42). Selected IR data ( $cm^{-1}$ , KBr pellet): 3416 (s, br,  $\nu(O-H)$  of  $H_2O$ ), 2924 [m,  $\nu(L^{2-})$ ], 1639 (m), 1600 [m,  $\nu(L^{2-})$ ], 1561 [m,  $\nu(L^{2-})$ ], 1507 [w,  $\nu(L^{2-})$ ], 1468 [s,  $\nu(L^{2-})$ ], 1386 (m), 1312 [m,  $\nu(Na-O)$ , O of  $H_2O$ ], 1265 [m,  $\nu(L^{2-})$ ], 1237 (w), 1149 (s), 1113 (s), 1090 [s,  $\nu(L^{2-})$ ], 938 [w,

$\nu(\text{Fe-O})$ ], 854 [m,  $\nu(\text{Fe-O}$  and  $L^{2-})$ ], 834 (w), 747 [m,  $\nu(L^{2-})$ ], 668 (w), 627 [m,  $\nu(\text{Fe-O})$ ], 564 (w), 481 [w,  $\nu(\text{Fe-N})$ ].

**[K<sub>3</sub>FeL<sub>3</sub>(H<sub>2</sub>O)<sub>5</sub>] (4).** A mixture of LH<sub>2</sub> (0.9 mmol, 0.146 g) and iron(III) perchlorate hydrate (0.3 mmol, 0.106 g) was added to a mixture of aqueous KOH solution (0.500 M, 2 mL) and DMF (2 mL) in a 10 mL vial. Slow evaporation of the solvents yielded a dark-purple solid within 2–3 weeks [68% yield, based on Fe(III)]. Anal. Calcd (Found) for K<sub>3</sub>C<sub>21</sub>H<sub>22</sub>N<sub>12</sub>O<sub>8</sub>Fe: C, 33.92 (33.19); H, 2.98 (3.17); N, 22.60 (22.38). Selected IR data (cm<sup>-1</sup>, KBr pellet): 3447 (s, br,  $\nu(\text{O-H}; \text{H}_2\text{O})$ ), 2925 [s,  $\nu(L^{2-})$ ], 2361 [m,  $\nu(\text{K-O})$ , O of H<sub>2</sub>O], 2345 [m,  $\nu(\text{K-O})$ , O of H<sub>2</sub>O], 1599 [s,  $\nu(L^{2-})$ ], 1560 [s,  $\nu(L^{2-})$ ], 1507 [m,  $\nu(L^{2-})$ ], 1467 [s,  $\nu(L^{2-})$ ], 1415 (m), 1384 [s,  $\nu(\text{K-O})$  and  $(L^{2-})$ ], 1312 [s,  $\nu(L^{2-})$ ], 1265 (m), 1244 (m), 1151 (m), 1111 [m,  $\nu(L^{2-})$ ], 1011 (m), 855 [m,  $\nu(\text{Fe-O})$  and  $(L^{2-})$ ], 751 [m,  $\nu(L^{2-})$ ], 670 (m), 609 [m,  $\nu(\text{Fe-O})$ ], 558 [m,  $\nu(\text{Fe-N})$ ].

**[K<sub>4</sub>Zn(FeL<sub>3</sub>)<sub>2</sub>(DMF)<sub>6</sub>] (5).** A mixture of LH<sub>2</sub> (0.9 mmol, 0.146 g), iron(III) perchlorate hydrate (0.3 mmol, 0.106 g), and zinc(II) perchlorate hydrate (0.15 mmol, 0.056 g) was added to a mixture of aqueous KOH solution (1.0 M, 2 mL) and DMF (2 mL) in a 10 mL vial and stirred for 5 h. All of the solvent was removed under vacuum, and the residue was redissolved in MeOH, followed by filtration to remove KClO<sub>4</sub>. Solvent was removed from the filtrate, and the residue was redissolved in DMF. Slow evaporation of the solvents yielded dark-purple crystals [74% yield, based on Fe(III)]. Anal. Calcd (Found) for C<sub>60</sub>H<sub>79</sub>Fe<sub>2</sub>K<sub>8</sub>N<sub>30</sub>O<sub>18</sub>Zn: C, 43.14 (43.25); H, 5.01 (5.08). Selected IR data (cm<sup>-1</sup>, KBr pellet): 3424 [s, br,  $\nu(\text{O-H})$  of H<sub>2</sub>O], 3198 [m, br,  $\nu(\text{K-O})$ , O of H<sub>2</sub>O], 2930 [w,  $\nu(\text{C-H})$ , DMF], 1658 [s,  $\nu(\text{C=O})$  of DMF], 1601 [m,  $\nu(\text{C=C})$ ,  $L^{2-}$ ], 1559 (m), 1511 (s), 1469 [s,  $\nu(\text{C=C})$ ,  $L^{2-}$ ], 1432 (m), 1391 (m), 1303 (s), 1265 (m), 1249 (m), 1106 (m), 853 [m,  $\nu(\text{Fe-O})$  and  $L^{2-}$ ], 762 (m), 671 (m), 60 [m,  $\nu(\text{Fe-O})$ ], 565 [w,  $\nu(\text{Fe-N})$ ], 422 [w,  $\nu(\text{Zn-N})$ ].

**X-ray Crystallography.** Diffraction data for complex **2** were measured at 100 K with synchrotron radiation ( $\lambda = 0.75000 \text{ \AA}$ ) using a 4AMXW ADSC Quantum-210 detector with a silicon double-crystal monochromator at the Pohang Accelerator Laboratory, Korea. HKL2000 (ver. 0.98.689)<sup>23</sup> was used for data collection, cell refinement, reduction, and absorption correction. Reflection data for **3–5** were collected using a Bruker APEX-II CCD-based diffractometer with graphite-monochromated Mo  $K\alpha$  radiation ( $\lambda = 0.7107 \text{ \AA}$ ). The hemisphere of reflection data was collected as  $\omega$  scan frames, with 0.5°/frame and an exposure time of 10 s/frame. Cell parameters were determined and refined using the SMART program.<sup>24</sup> Data reduction was performed using SAINT software.<sup>25</sup> Data were corrected for Lorentz and polarization effects. An empirical absorption correction was applied using the SADABS program.<sup>26</sup> The structures of the compounds were solved by direct methods and refined by the full-matrix least-squares method using the SHELXTL program package with anisotropic thermal parameters for all non-hydrogen atoms.<sup>27</sup> CCDC structures 974366–974369 contain crystallographic data for compounds **2–5**. These data can be obtained free of charge from The Cambridge Crystallographic Data Centre via [www.ccdc.cam.ac.uk/data\\_request/cif](http://www.ccdc.cam.ac.uk/data_request/cif).

**Cyclic Voltammetry.** CV measurements were carried out with a three-electrode cell configuration consisting of platinum working and counter electrodes and a Ag/AgCl (manufactured by BASi, MF-2052, 3.0 M NaCl) reference electrode at room temperature. Redox potentials were recorded at a scan rate of 200 mV/s. Experiments were carried out with 1 mg of sample in an argon-saturated tetra-*n*-butylammonium hexafluorophosphate (0.1 M) MeCN solution.

**Titration Experiments.** UV–vis absorption measurements for alkali metal ions with complex **1** were performed in MeCN using a 1 cm quartz cuvette at ambient temperature. A solution of **1** (3.0 mL, 5.0  $\times 10^{-5}$  M, MeCN) was titrated with incremental amounts of alkali metal ion perchlorate (M = Li, Na, and K). The initial  $\lambda_{\text{max}}$  of **1** was 433 nm. The peak shifted to longer wavelength on addition of alkali metal ion perchlorate solution (433  $\rightarrow$  483 nm).

**X-ray Photoelectron Spectroscopy.** XPS analysis was conducted using a VG Multilab 2000 spectrometer (ThermoVG Scientific) in an ultrahigh vacuum, which utilizes an unmonochromatized Mg  $K\alpha$  (1253.6 eV) source and a spherical section analyzer. The accuracy of

the binding energy (BE) values was  $\pm 0.1$  eV. In the analysis of the XPS peaks, the BEs were corrected for specimen charging by referencing the C 1s peak to 284.6 eV. The background was subtracted by Shirley's method, and spectrum deconvolution was accomplished by Voigt-profile fitting.

## ■ ASSOCIATED CONTENT

### 📄 Supporting Information

UV and mass spectra and X-ray data for compounds **2–5**, CV data for **2–4**, SQUID data for **3** and **4**, and Job's plot data. This material is available free of charge via the Internet at <http://pubs.acs.org>.

## ■ AUTHOR INFORMATION

### Corresponding Authors

\*E-mail: [ykim@chungbuk.ac.kr](mailto:ykim@chungbuk.ac.kr).

\*E-mail: [leespy@chonnam.ac.kr](mailto:leespy@chonnam.ac.kr).

### Author Contributions

‡These authors contributed equally.

### Notes

The authors declare no competing financial interest.

## ■ ACKNOWLEDGMENTS

We acknowledge support from the Basic Science Research Program through the National Research Foundation of Korea (NRF), funded by the Ministry of Education, Science, and Technology (NRF-2010-0003141 and NRF-2013R1A1A2006317).

## ■ REFERENCES

- (1) (a) Trofimenko, S. *Polyhedron* **2004**, *23*, 197–203. (b) Paulo, A.; Correia, J. D. G.; Campello, M. P. C.; Santos, I. *Polyhedron* **2004**, *23*, 331–360. (c) Pettinari, C.; Cingolani, A.; Lobbia, G. G.; Marchetti, F.; Martini, D.; Pellei, M.; Pettinari, R.; Santini, C. *Polyhedron* **2004**, *23*, 451–469. (d) Hamon, P.; Thepot, J. Y.; Le Floch, M.; Boulon, M. E.; Cador, O.; Golhen, S.; Ouahab, L.; Fadel, L.; Saillard, J. Y.; Hamon, J. R. *Angew. Chem., Int. Ed.* **2008**, *47*, 8687–8691. (e) Edelmann, F. T. *Angew. Chem., Int. Ed.* **2001**, *40*, 1656–1660. (f) Reger, D. L.; Gardinier, J. R.; Gemmill, W. R.; Smith, M. D.; Shahin, A. M.; Long, G. J.; Rebbouh, L.; Grandjean, F. *J. Am. Chem. Soc.* **2005**, *127*, 2303–2316. (g) Reger, D. L.; Collins, J. E.; Rheingold, A. L.; Liable-Sands, L. M. *Inorg. Chem.* **1999**, *38*, 3235–3237. (h) Reger, D. L.; Elgin, J. D.; Foley, E. A.; Smith, M. D.; Grandjean, F.; Long, G. J. *Inorg. Chem.* **2009**, *48*, 9393–9401.
- (2) (a) Cheng, J.; Saliu, K.; Kiel, G. Y.; Ferguson, M. J.; McDonald, R.; Takats, J. *Angew. Chem., Int. Ed.* **2008**, *47*, 4910–4913. (b) Otero, A.; Fernandez-Baeza, J.; Lara-Sanchez, A.; Antinolo, A.; Tejada, J.; Martinez-Caballero, E.; Marquez-Segovia, I.; Lopez-Solera, I.; Sanchez-Barba, L. F.; Alonso-Moreno, C. *Inorg. Chem.* **2008**, *47*, 4996–5005. (c) Müller, M.; Lork, E.; Mews, R. *Angew. Chem., Int. Ed.* **2001**, *40*, 1247–1249.
- (3) Guo, S. L.; Peters, F.; de Biani, F. F.; Bats, J. W.; Herdtweck, E.; Zanello, P.; Wagner, M. *Inorg. Chem.* **2001**, *40*, 4928–4936.
- (4) Jernigan, F. E.; Sieracki, N. A.; Taylor, M. T.; Jenkins, A. S.; Engel, S. E.; Rowe, B. W.; Jove, F. A.; Yap, G. P. A.; Papish, E. T.; Ferrence, G. M. *Inorg. Chem.* **2007**, *46*, 360–362.
- (5) (a) Silva, R. M.; Gwengo, C.; Lindeman, S. V.; Smith, M. D.; Gardinier, J. R. *Inorg. Chem.* **2006**, *45*, 10998–11007. (b) Rabinovich, D. *Struct. Bonding (Berlin)* **2006**, *120*, 143–162.
- (6) Blagg, R. J.; Adams, C. J.; Charmant, J. P. H.; Connelly, N. G.; Haddow, M. F.; Hamilton, A.; Knight, J.; Orpen, A. G.; Ridgway, B. M. *Dalton Trans.* **2009**, 8724–8736.
- (7) Silva, R. M.; Gwengo, C.; Lindeman, S. V.; Smith, M. D.; Long, G. J.; Grandjean, F.; Gardinier, J. R. *Inorg. Chem.* **2008**, *47*, 7233–7242.



(8) (a) Bond, A. D.; Fleming, A.; Gaire, J.; Kelleher, F.; McGinley, J.; McKee, V.; Sheridan, U. *Polyhedron* **2012**, *33*, 289–296. (b) Nouar, F.; Eubank, J. F.; Bousquet, T.; Wojtas, L.; Zaworotko, M. J.; Eddaoudi, M. *J. Am. Chem. Soc.* **2008**, *130*, 1833–1835.

(9) (a) Sengupta, O.; Mukherjee, P. S. *Inorg. Chem.* **2010**, *49*, 8583–8590. (b) Rodriguez, A.; Kivekas, R.; Colacio, E. *Chem. Commun.* **2005**, 5228–5230.

(10) (a) Hassan, N.; Stelzl, J.; Weinberger, P.; Molnar, G.; Bousseksou, A.; Kubel, F.; Mereiter, K.; Boca, R.; Linert, W. *Inorg. Chim. Acta* **2013**, *396*, 92–100. (b) Yan, Z.; Li, M.; Gao, H. L.; Huang, X. C.; Li, D. *Chem. Commun.* **2012**, *48*, 3960–3962.

(11) (a) Cui, P.; Ma, Y. G.; Li, H. H.; Zhao, B.; Li, J. R.; Cheng, P.; Balbuena, P. B.; Zhou, H. C. *J. Am. Chem. Soc.* **2012**, *134*, 18892–18895. (b) Hu, T. P.; Liu, L. J.; Lv, X. L.; Chen, X. H.; He, H. Y.; Dai, F. N.; Zhang, G. Q.; Sun, D. F. *Polyhedron* **2010**, *29*, 296–302.

(12) Hill, M. S.; Hitchcock, P. B.; Smith, N. *Polyhedron* **2004**, *23*, 801–807.

(13) (a) Janiak, C.; Scharmann, T. G.; Gunther, W.; Girgsdies, F.; Hemling, H.; Hinrichs, W.; Lentz, D. *Chem.—Eur. J.* **1995**, *1*, 637–644. (b) Janiak, C.; Scharmann, T. G.; Brzezinka, K. W.; Reich, R. *Chem. Ber.* **1995**, *128*, 323–328. (c) Janiak, C. *J. Chem. Soc., Chem. Commun.* **1994**, 545–547. (d) Janiak, C.; Esser, L. *Z. Naturforsch. B* **1993**, *48*, 394–396. (e) Janiak, C.; Scharmann, T. G. *Polyhedron* **2003**, *22*, 1123–1133. (f) Groshens, T. J. *J. Coord. Chem.* **2010**, *63*, 1882–1892. (g) Lu, D. M.; Winter, C. H. *Inorg. Chem.* **2010**, *49*, 5795–5797.

(14) Snyder, C. J.; Martin, P. D.; Heeg, M. J.; Winter, C. H. *Chem.—Eur. J.* **2013**, *19*, 3306–3310.

(15) Go, M. J.; Lee, K. M.; Oh, C. H.; Kang, Y. Y.; Kim, S. H.; Park, H. R.; Kim, Y.; Lee, J. *Organometallics* **2013**, *32*, 4452–4455.

(16) Koguro, K.; Oga, T.; Mitsui, S.; Orita, R. *Synthesis* **1998**, 910–914.

(17) (a) Shongwe, M. S.; Al-Rashdi, B. A.; Adams, H.; Morris, M. J.; Mikuriya, M.; Hearne, G. R. *Inorg. Chem.* **2007**, *46*, 9558–9568. (b) Strautmann, J. B. H.; George, S. D.; Bothe, E.; Bill, E.; Weyhermüller, T.; Stammler, A.; Bögge, H.; Glaser, T. *Inorg. Chem.* **2008**, *47*, 6804–6824. (c) Heistand, R. H.; Lauffer, R. B.; Fikrig, E.; Que, L. *J. Am. Chem. Soc.* **1982**, *104*, 2789–2796.

(18) Harding, D. J.; Sertphon, D.; Harding, P.; Murray, K. S.; Moubaraki, B.; Cashion, J. D.; Adams, H. *Chem.—Eur. J.* **2013**, *19*, 1082–1090.

(19) Lehnert, N.; Ho, R. Y. N.; Que, L.; Solomon, E. I. *J. Am. Chem. Soc.* **2001**, *123*, 12802–12816.

(20) Shannon, R. *Acta Crystallogr., Sect. A* **1976**, *32*, 751–767.

(21) Chisholm, M. H.; Gallucci, J. C.; Yaman, G. *Chem. Commun.* **2006**, 1872–1874.

(22) Bhattacharjee, C. R.; Goswami, P.; Mondal, P. *Inorg. Chim. Acta* **2012**, *387*, 86–92.

(23) Otwinowski, Z.; Minor, W. *Methods in Enzymology*; Carter, C.W., Jr.; Sweet, R. M., Eds.; Academic Press: New York, 1997; , Vol. 276, pp 307–326.

(24) SMART, version 5.0; Bruker AXS, Inc.: Madison, WI, 1998.

(25) SAINT, version 5.0; Bruker AXS Inc.: Madison, WI, 1998.

(26) Sheldrick, G. M. *SADABS*; University of Gottingen: Gottingen, Germany, 1996.

(27) Sheldrick, G. M. *SHELXS-97*; University of Gottingen: Gottingen, Germany, 1997.